

# Phase Transition in Perovskite Manganites with Orbital Degree of Freedom

S. Okamoto, S. Ishihara, and S. Maekawa

*Institute for Materials Research, Tohoku University, Sendai 980-8577, Japan*

(May 16, 2018)

Roles of orbital degree of freedom of Mn ions in phase transition as a function of temperature and hole concentration in perovskite manganites are studied. It is shown that the orbital order-disorder transition is of the first order in the wide region of hole concentration and the Néel temperature for the anisotropic spin ordering, such as the layer-type antiferromagnetic one, is lower than the orbital ordering temperature due to the anisotropy in the orbital space. The calculated results of the temperature dependence of the spin and orbital order parameters explain a variety of the experiments observed in manganites.

PACS numbers: 75.30.Vn, 71.30.+h, 75.30.Kz, 75.30.Et

## I. INTRODUCTION

Perovskite manganites  $A_{1-x}B_x\text{MnO}_3$  ( $A$ : La, Nd, Pr,  $B$ : Sr, Ca) and their related compounds have been recently studied extensively from both experimental and theoretical sides. Anomalous electric, magnetic and structural properties accompanied with the phase transition such as colossal magnetoresistance (CMR) attract much attention.<sup>1-4</sup> Gigantic decrease of the electrical resistivity is brought about at the vicinity of the transition from spin, charge and orbital ordered phase to ferromagnetic metallic one with slightly changing temperature and/or applying external fields.<sup>5,6</sup> It is now accepted that such dramatic phenomena are not understood within the simple double exchange scenario.<sup>7</sup>

The orbital degree of freedom in Mn ions is one of the convincing candidates to bring about not only a rich variety of phenomena but also dramatic ones. Due to the strong Hund coupling and the crystalline field, two  $e_g$  orbitals of a Mn ion, i.e. the  $d_{3z^2-r^2}$  and  $d_{x^2-y^2}$  orbitals, are degenerate and one of them is occupied by an electron in a  $\text{Mn}^{3+}$  ion. It is well known that the  $(d_{3z^2-r^2}/d_{3y^2-r^2})$ -type orbital ordered state, where the two orbitals are alternately aligned, is realized in the undoped manganites  $\text{LaMnO}_3$ .<sup>8-12</sup> After the discovery of CMR, much study of the orbital states in doped manganites has been done. For example, the layer (A)-type antiferromagnetic (AF) metal accompanied with the uniform alignment of the  $d_{x^2-y^2}$  orbital is observed in  $\text{Pr}_{0.5}\text{Sr}_{0.5}\text{MnO}_3$ ,  $\text{Nd}_{0.45}\text{Sr}_{0.55}\text{MnO}_3$ <sup>13-15</sup> and  $\text{La}_{1-x}\text{Sr}_x\text{MnO}_3$  with  $x \sim 0.55$ .<sup>16</sup> Nevertheless, roles of the orbital in phase transition are still far from our understanding. Since CMR appears near the orbital order-disorder transition, it is indispensable to study nature of the phase transition in doped manganites where the orbital degree of freedom is taken into account.

In this paper, we study the phase transition in perovskite manganites based on the model where the orbital degree of freedom and electron correlation are included. By adopting the mean field theory, the phase transitions are investigated as a functions of temperature ( $T$ ) and carrier concentration ( $x$ ). Since there is a strong anisotropy in the orbital space unlike the spin one,

the orbital order-disorder transition is of the first order in the wide range of  $x$ , and the Néel temperature  $T_N$  for the anisotropic spin ordering, such as the A-type AF one, is lower than the orbital ordering temperature  $T_{OO}$ . The calculated temperature dependence of the spin and orbital order parameters explains a variety of experiments in several manganites.

In Sect. II, the model Hamiltonian is derived and the mean field theory at finite  $T$  is introduced. In Sect. III, the numerical results of the spin and orbital phase diagram are presented. We focus on the phase transitions in (i) lightly doped region where the ferromagnetic Curie temperature,  $T_C$ , and  $T_{OO}$  are close with each other and (ii) highly doped one where the A-type AF state accompanied with the  $d_{x^2-y^2}$  orbital appears. In Sect. IV, phase transition is studied analytically by expanding the free energy with respect to the spin and orbital order parameters. Section V is devoted to the summary and discussion.

## II. MODEL AND FORMULATION

Let us set up the model Hamiltonian describing the electronic structure in manganites. We consider the tight-binding Hamiltonian in the cubic lattice consisting of Mn ions. At each site, two  $e_g$  orbitals are introduced and  $t_{2g}$  electrons are treated as a localized spin ( $\vec{S}_{t_{2g}}$ ) with  $S = 3/2$ . We introduce three kinds of Coulomb interaction between  $e_g$  electrons at the same site, i.e. the intra-orbital Coulomb interaction ( $U$ ), the inter-orbital one ( $U'$ ) and the exchange interaction ( $I$ ). The hopping integral between site  $i$  with orbital  $\gamma$  and its nearest neighboring site  $j$  with  $\gamma'$  is denoted by  $t_{ij}^{\gamma\gamma'}$ . The Hund coupling ( $J_H$ ) between  $e_g$  and  $t_{2g}$  spins and the antiferromagnetic superexchange (SE) interaction ( $J_{AF}$ ) between nearest neighboring  $t_{2g}$  spins are also introduced. Among these parameters, the intra-site Coulomb interactions are the largest. Thus, by excluding the doubly occupied state in the  $e_g$  orbitals, we derive the effective Hamiltonian describing the low energy electronic states:<sup>17</sup>

$$\mathcal{H} = \mathcal{H}_t + \mathcal{H}_J + \mathcal{H}_H + \mathcal{H}_{AF}. \quad (1)$$

The first and second terms correspond to the so-called  $t$ - and  $J$ -terms in the  $tJ$ -model and are given by

$$\mathcal{H}_t = \sum_{\langle ij \rangle \gamma \gamma' \sigma} t_{ij}^{\gamma \gamma'} \tilde{d}_{i\gamma\sigma}^\dagger \tilde{d}_{j\gamma'\sigma} + H.c., \quad (2)$$

and

$$\begin{aligned} \mathcal{H}_J &= -2J_1 \sum_{\langle ij \rangle} \left( \frac{3}{4} n_i n_j + \vec{S}_i \cdot \vec{S}_j \right) \left( \frac{1}{4} - \tau_i^l \tau_j^l \right) \\ &\quad - 2J_2 \sum_{\langle ij \rangle} \left( \frac{1}{4} n_i n_j - \vec{S}_i \cdot \vec{S}_j \right) \left( \frac{3}{4} + \tau_i^l \tau_j^l + \tau_i^l + \tau_j^l \right), \quad (3) \end{aligned}$$

respectively. Here,  $\tau_i^l = \cos(\frac{2\pi}{3} m_l) T_{iz} - \sin(\frac{2\pi}{3} m_l) T_{ix}$  and  $(m_x, m_y, m_z) = (1, -1, 0)$ .  $l$  denotes a direction of the bond connecting site  $i$  and site  $j$ .  $\tilde{d}_{i\gamma\sigma}$  is the annihilation operator of the  $e_g$  electron at site  $i$  with spin  $\sigma$  and orbital  $\gamma$  with excluding double occupancy of electron and  $n_i$  is the number operator defined as  $n_i = \sum_{\gamma\sigma} \tilde{d}_{i\gamma\sigma}^\dagger \tilde{d}_{i\gamma\sigma}$ . The explicit form of  $t_{ij}^{\gamma \gamma'}$  is determined by the Slater-Koster formulas.<sup>18</sup>  $\vec{S}_i$  is the spin operator of the  $e_g$  electron with  $S = 1/2$  and  $\vec{T}_i$  is the pseudo-spin one for the orbital degree of freedom defined as  $\vec{T}_i = (1/2) \sum_{\gamma\gamma'\sigma} \tilde{d}_{i\gamma\sigma}^\dagger (\vec{\sigma})_{\gamma\gamma'} \tilde{d}_{i\gamma'\sigma}$  where  $T_{iz} = +(-)1/2$  corresponds to the state where the  $d_{3z^2-r^2}$  ( $d_{x^2-y^2}$ ) orbital is occupied by an electron.  $J_1 = t_0^2/(U' - I)$  and  $J_2 = t_0^2/(U' + I + 2J_H)$  where  $t_0$  is the hopping integral between nearest neighboring  $d_{3z^2-r^2}$  orbitals in the  $z$  direction and  $U = U' + I$  is assumed. The third and fourth terms in Eq. (1) represent the Hund coupling and the antiferromagnetic SE interaction, respectively, and are given by

$$\begin{aligned} \mathcal{H}_H + \mathcal{H}_{AF} &= -J_H \sum_i \vec{S}_i \cdot \vec{S}_{t_{2g}i} \\ &\quad + J_{AF} \sum_{\langle ij \rangle} \vec{S}_{t_{2g}i} \cdot \vec{S}_{t_{2g}j}. \quad (4) \end{aligned}$$

The detailed derivation of the Hamiltonian is presented in Ref. 17. Characteristics of this Hamiltonian are summarized as follows; 1) the two kinds of magnetic interactions between spins of  $e_g$  electrons, i.e. the SE and double exchange interactions are described by  $\mathcal{H}_J$  and  $\mathcal{H}_t$ , respectively,<sup>19</sup> 2) there is a strong anisotropy in the pseudo-spin space unlike the spin space, and 3) the first term in Eq. (3) is the dominant term in  $\mathcal{H}_J$  and stabilizes the ferromagnetic state associated with the antiferro-type orbital ordered one where different types of orbital are alternately aligned.<sup>20-23</sup>

Being based on the Hamiltonian, the spin and orbital states are studied at finite  $T$  and  $x$ . The mean field theory proposed by de Gennes<sup>24</sup> is applied to the present system with orbital degeneracy and electron correlation.<sup>25</sup> In this theory, the spin and pseudo-spin operators are treated as classical vectors:

$$(S_{ix}, S_{iy}, S_{iz}) = \frac{1}{2} (\sin \theta_i^s \cos \phi_i^s, \sin \theta_i^s \sin \phi_i^s, \cos \theta_i^s), \quad (5)$$

and

$$(T_{ix}, T_{iy}, T_{iz}) = \frac{1}{2} (\sin \theta_i^t, 0, \cos \theta_i^t), \quad (6)$$

where  $\theta_i^{s(t)}$  is the polar angle in the spin (orbital) space and  $\phi_i^s$  is the azimuthal one in the spin space. A motion of the pseudo-spin is assumed to be confined in the  $xz$  plane and  $\theta_i^t$  describes the orbital state at site  $i$  as follows

$$|\theta_i^t\rangle = \cos \frac{\theta_i^t}{2} |3z^2 - r^2\rangle + \sin \frac{\theta_i^t}{2} |x^2 - y^2\rangle. \quad (7)$$

From now on,  $\vec{S}_i$  and  $\vec{T}_i$  are denoted by  $\vec{u}_i$  in the uniform fashion. A thermal distribution of  $\vec{u}_i$  is described by the distribution function:

$$w_i^u(\vec{u}_i) = \frac{1}{\nu_i^u} \exp\left(\vec{\lambda}_i^u \cdot \frac{\vec{u}_i}{|\vec{u}_i|}\right), \quad (8)$$

where  $\vec{\lambda}_i^u$  is the mean field and  $\nu_i^u$  is the normalization factor given by

$$\nu_i^s = \int_0^\pi d\theta_i^s \int_0^{2\pi} d\phi_i^s \sin \theta_i^s \exp(|\vec{\lambda}_i^s| \cos \theta_i^s), \quad (9)$$

and

$$\nu_i^t = \int_0^{2\pi} d\theta_i^t \exp(|\vec{\lambda}_i^t| \cos \theta_i^t). \quad (10)$$

The free energy is given by a summation of the expectation value of the Hamiltonian and entropy:

$$\mathcal{F} = \langle \mathcal{H} \rangle_{st} - TN(\mathcal{S}^s + \mathcal{S}^t), \quad (11)$$

where  $N$  is the number of Mn ions and  $\mathcal{S}^u$  is the entropy for  $\vec{u}$  defined by

$$\mathcal{S}^u = -\langle \ln w^u(\vec{u}) \rangle_u. \quad (12)$$

$\langle A \rangle_u$  implies the expectation value of  $A$  with respect to the distribution function.  $M_u = \langle \vec{u} \cdot \vec{\lambda}^u / (|\vec{u}| |\vec{\lambda}^u|) \rangle_u$  is adopted as an order parameter in  $\langle \mathcal{H}_J \rangle_{st}$ ,  $\langle \mathcal{H}_H \rangle_{st}$  and  $\langle \mathcal{H}_{AF} \rangle_{st}$ . The relation  $3\langle \vec{S}_i \rangle_s = \langle \vec{S}_{t_{2g}i} \rangle_s$  is assumed. As for  $\langle \mathcal{H}_t \rangle_{st}$ , the rotating frames in the spin and pseudo-spin spaces are introduced. The electron annihilation operator is decomposed as  $\tilde{d}_{i\gamma\sigma} = z_{i\sigma}^s z_{i\gamma}^t h_i^\dagger$  where  $h_i^\dagger$  is the creation operator of a spin- and orbital-less fermion describing a hole motion and  $z_{i\sigma}^{s(t)}$  is an element of the unitary matrix in the spin (pseudo-spin) frame.<sup>26,27</sup> These are given by  $z_{i\uparrow}^s = \cos(\theta_i^s/2) e^{-i\phi_i^s/2}$ ,  $z_{i\downarrow}^s = \sin(\theta_i^s/2) e^{i\phi_i^s/2}$ ,  $z_{ia}^t = \cos(\theta_i^t/2)$  and  $z_{ib}^t = \sin(\theta_i^t/2)$ .  $\mathcal{H}_t$  is rewritten as

$$\mathcal{H}_t = \sum_{\langle ij \rangle \sigma \gamma \gamma'} (z_{i\sigma}^{s*} z_{j\sigma}^s) (z_{i\gamma}^{t*} z_{j\gamma'}^t) z_{j\gamma'}^\dagger h_j^\dagger + H.c., \quad (13)$$

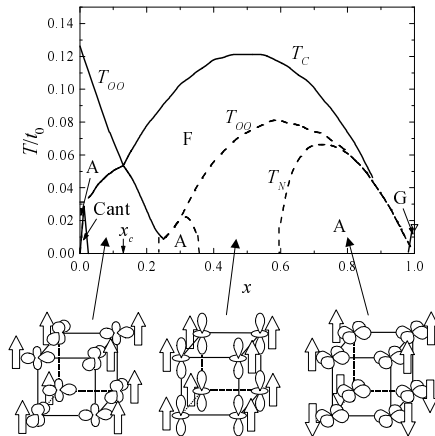


FIG. 1. The spin and orbital phase diagram as a function of hole concentration ( $x$ ) and temperature ( $T$ ). The schematic orbital states are also shown.  $T_C$ ,  $T_N$  and  $T_{OO}$  indicate ferromagnetic Curie temperature, Néel temperature and orbital ordering temperature, respectively.  $F$ ,  $A$  and  $G$  indicate ferromagnetic, A-type antiferromagnetic and G-type antiferromagnetic phases, respectively. The solid (broken) lines are for the second (first) order phase transition. The parameter values are chosen to be  $J_1/t_0 = 0.25$ ,  $J_2/t_0 = 0.075$ , and  $J_{AF}/t_0 = 0.0035$ .

and is diagonalized in the momentum space as follows

$$\langle \mathcal{H}_t \rangle_{st} = \left\langle \sum_{\vec{k}} \sum_{l=1}^{N_l} \varepsilon_{\vec{k}}^l f_F(\varepsilon_{\vec{k}}^l - \varepsilon_F) \right\rangle_{st}, \quad (14)$$

where  $\varepsilon_{\vec{k}}^l$  is the energy in the  $l$ -th band for the spin- and orbital-less fermion with momentum  $\vec{k}$  and  $N_l$  is the number of the band. The Fermi energy  $\varepsilon_F$  is determined by the condition  $x = (1/N) \sum_{\vec{k}} \sum_l f_F(\varepsilon_{\vec{k}}^l - \varepsilon_F)$  where  $f_F(\varepsilon)$  is the Fermi distribution function. The mean field solutions are obtained by minimizing  $\mathcal{F}$  with respect to  $\tilde{\lambda}_i^u$ .

### III. NUMERICAL RESULTS

#### A. spin and orbital phase diagram at finite temperature

The spin and orbital states at finite  $T$  and  $x$  are numerically calculated by utilizing the mean field theory introduced in the previous section. The four types of spin structure, that is, the ferromagnetic (F) structure and layer (A)-type, rod (C)-type and NaCl (G)-type AF ones are considered. As for the orbital, the ferromagnetic-like structure where one kind of orbital exists and the G-type one where two kinds of orbital are alternately aligned in the [111] direction are considered. The numerical results are shown in Fig. 1. Parameter values are chosen to be  $J_1/t_0 = 0.25$ ,  $J_2/t_0 = 0.075$  and  $J_{AF}/t_0 = 0.0035$ .

The schematic pictures of the orbital ordered states are also presented. With increasing  $x$  from  $x = 0$ , the spin structure changes as A-type AF  $\rightarrow$  F  $\rightarrow$  A-type AF  $\rightarrow$  G-type AF which is associated with change of the orbital states; in the region of  $x \leq 0.25$ , the interaction caused by  $\mathcal{H}_J$  is the dominant one between nearest neighboring orbitals and the G-type AF orbital ordered state is brought about. The type of the orbital is denoted as  $(\Theta_A^t/\Theta_B^t) = (\frac{\pi}{2}/-\frac{\pi}{2})$  where  $\Theta_{A(B)}^t$  is the angle of the pseudo-spin in sublattice  $A(B)$  and its definition is the same with  $\theta_i^t$  in Eq. (7). These orbitals are mixtures of  $d_{3x^2-r^2}$  and  $d_{y^2-z^2}$ , and  $d_{3y^2-r^2}$  and  $d_{z^2-x^2}$ , respectively. Above  $x = 0.25$ , the F-type orbital ordered state is realized. In particular, the  $d_{x^2-y^2}$  orbital is uniformly aligned in the A-type AF spin phase above  $x = 0.6$ . A large hopping integral for electrons in the  $xy$  plane in this orbital ordered state is energetically favored in the A-type AF state where the hopping in the  $z$  direction is prohibited.<sup>28</sup> The calculated results of spin and orbital phase diagram at  $T = 0$  are consistent with those obtained by the Hartree-Fock theory.<sup>28</sup> The spin and orbital phase diagram at finite  $T$  was calculated in Ref. 29 where the Monte Carlo method in a finite-size cluster was used in the spin-orbital-lattice coupled model.

Now, let us focus on the spin ordering temperatures, i.e.  $T_C$  and  $T_N$ , and the orbital ordering one,  $T_{OO}$ , in Fig. 1. These ordering temperature vs.  $x$  curves qualitatively reproduce the experimental results observed in  $\text{La}_{1-x}\text{Sr}_x\text{MnO}_3$ ,<sup>30,16</sup>  $\text{Pr}_{1-x}\text{Sr}_x\text{MnO}_3$ <sup>30,15</sup> and  $\text{Nd}_{1-x}\text{Sr}_x\text{MnO}_3$ <sup>14</sup> except for the narrow region of the charge ordered phase in  $\text{Nd}_{0.5}\text{Sr}_{0.5}\text{MnO}_3$ . It is shown in Fig. 1 that  $T_{OO}$  is higher (lower) than  $T_C$  in the region of  $x < 0.1$  ( $x > 0.1$ ). The dominant interaction in the region of  $x < 0.1$  is provided by  $\mathcal{H}_J$  where the effective interaction between orbitals in the paramagnetic state and that between spins in the orbital disordered state are given by  $3J_1/2$  and  $J_1/2$ , respectively. Here, the first term in  $\mathcal{H}_J$  is considered. Thus,  $T_{OO}$  is higher than  $T_C$ . On the other hand, in the region where  $\mathcal{H}_t$  is dominant, gain of the kinetic energy associated with the long range ordering causes the transition; it is assumed that doped holes are introduced at the bottom of the band and the kinetic energy is proportional to the band width. The ratio of the band width in the ferromagnetic state to that in the paramagnetic one is obtained as  $3/2$  where the orbital disordered state is assumed. On the other hand, the ratio of the band width in the F-type orbital ordered state to that in the orbital disordered state is obtained as  $\pi^2/8$  where the spin paramagnetic state is assumed. The energy gain associated with the orbital ordering is smaller than that with the spin one, so that  $T_C$  is higher than  $T_{OO}$ . This is attributed to the hopping integral between different kinds of orbital.

Between  $T_N$  for the A-type AF state and  $T_{OO}$ , the relation  $T_N \leq T_{OO}$  is satisfied in the whole region of  $x$  in Fig. 1. In addition, the orbital order-disorder transition and the A-type AF one are of the first order in the region

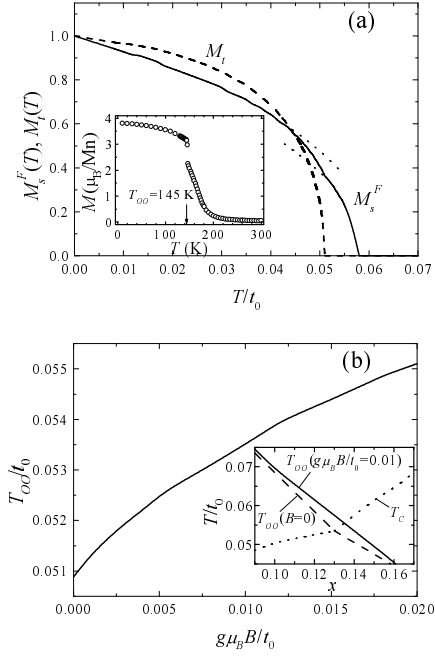


FIG. 2. (a) Temperature dependence of the magnetization  $M_s^F$  (solid line) and the orbital order parameter  $M_t$  (broken line) at  $x = 0.14$ . The inset shows the magnetization curve in  $\text{La}_{0.88}\text{Sr}_{0.12}\text{MnO}_3$ .<sup>31</sup> (b) Magnetic field dependence of the orbital ordering temperature  $T_{OO}$  at  $x = 0.14$ . The inset shows  $T_{OO}$  at  $g\mu_B B/t_0 = 0$  and 0.01 and the ferromagnetic Curie temperature  $T_C$  around  $x_c$ . Parameter values in the calculation are the same as those in Fig. 1.

of  $x > 0.25$ . This is numerically confirmed by discontinuity in the orbital (spin) order parameter at  $T_{OO}$  ( $T_N$ ). Both the two results originate from the anisotropy in the pseudo-spin space as discussed latter in more detail.

### B. spin and orbital phase transitions in lightly doped region

In the lightly doped region in Fig. 1,  $T_C$  ( $T_{OO}$ ) increases (decreases) with increasing  $x$  from  $x = 0$  and the two transition temperatures cross with each other around  $x = 0.13$  termed  $x_c$ . Around  $x_c$ , the coupling between spin and orbital degrees of freedom brings about the unique phase transition as follows. Let us focus on the region where  $x$  is slightly higher than  $x_c$ . With decreasing  $T$ , the system changes from the paramagnetic phase with the orbital disordered state to the ferromagnetic phase and then to the ferromagnetic one with the orbital ordered state. The temperature dependence of the magnetization at  $x = 0.14$  is presented in Fig. 2 (a) where the order parameter of the orbital ordered state is also plotted. It is shown that the magnetization is enhanced below  $T_{OO}$ . This originates from the coupling between spin and orbital in  $\mathcal{H}_J$  (Eq. (3)); in the mean fields theory, the effective interaction between nearest

neighboring spins is given by  $-2J_1(\langle n_i n_j \rangle / 4 - \langle \tau_i^l \tau_j^l \rangle)$  where the first term in  $\mathcal{H}_J$  is considered. With taking into account the fact that the orbital ordered state is  $(\Theta_A, \Theta_B) = (\pi/3, 3\pi/2)$  in this region of  $x$ , the effective interaction is rewritten as  $-2J_1(1-x)^2(1/4 + 3M_t^2/16)$  for  $l = x$  and  $y$  and  $-2J_1(1-x)^2/4$  for  $l = z$ . The effective magnetic interaction and thus the magnetization increase below  $T_{OO}$ . In the opposite way, the orbital order-disorder transition is influenced by change of the spin state. The magnetic field dependence of  $T_{OO}$  at  $x = 0.14$  is presented in Fig. 2 (b). The inset shows change of the phase diagram by applying the magnetic field around  $x_c$ .  $T_{OO}$  increases with applying a magnetic field. The effective interaction between nearest neighboring orbitals is given by  $2J_1(1-x)^2(3/4 + M_s^2/4)$  which increases by applying the magnetic field. This implies that the orbital state is controlled by the magnetic field, although the field is not a canonical external field for the pseudo-spin.

This unique phase transition originating from the coupling between spin and orbital is observed in manganites.<sup>19,31</sup> In  $\text{La}_{0.88}\text{Sr}_{0.12}\text{MnO}_3$ , the ferromagnetic ordering occurs at 175K and the orbital ordering is confirmed below 145K by the resonant x-ray scattering which is a direct probe to detect the orbital ordering. The ferromagnetic phase with the orbital disordered state changes into the phase with the orbital ordered state at 145K, so that it corresponds to the calculated phase transition at  $T_{OO}$  around  $x = 0.14$ . It is experimentally confirmed that the magnetization is enhanced below 145K (the inset of Fig. 2(a)) and the orbital ordering temperature increases with applying the magnetic field.<sup>32-34,31</sup> These experimental results are well explained by the present calculation and are strong evidences of the novel coupling between spin and orbital in this compound.

### C. phase transition in highly doped region and A-type AF metal

In this subsection, we focus on the phase transition in the highly doped region ( $x > 0.5$ ) in Fig. 1 where the A-type AF state associated with the  $d_{x^2-y^2}$  orbital ordered one appears. There are two kinds of carrier concentration regions termed region I ( $0.8 > x > 0.6$ ) where a sequential phase transition from the paramagnetic state to the ferromagnetic one and to the A-type AF one occurs with decreasing  $T$ , and region II ( $x > 0.8$ ) where the transition from the paramagnetic state to the A-type AF one occurs. The temperature dependences of the spin order parameters at  $x = 0.725$  (region I) and  $x = 0.9$  (region II) are shown in Figs. 3(a) and (b), respectively.  $M_s^F$  and  $M_s^{AF}$  are the order parameters of the ferromagnetic and A-type AF spin structures, respectively. As shown in Fig. 3(a),  $M_s^F$  appears at  $T_C/t_0 = 0.95$  where the transition is of the second order. With decreasing  $T$ , the F-type orbital ordered state with  $d_{x^2-y^2}$  orbital appears

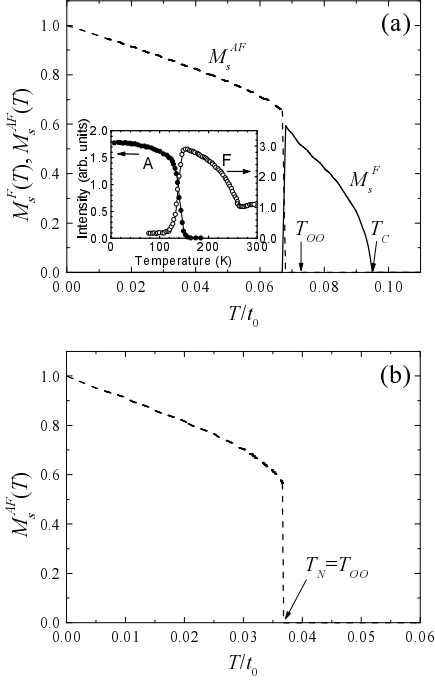


FIG. 3. Temperature dependences of the spin order parameters (a) at  $x = 0.725$  and (b) at  $x = 0.9$ . The solid and broken lines show the order parameters in the ferromagnetic state ( $M_s^F$ ) and the A-type antiferromagnetic one ( $M_s^{AF}$ ), respectively. Parameter values are the same as those in Fig. 1. The inset in (a) shows the temperature dependences of magnetic Bragg reflections in  $\text{Pr}_{0.5}\text{Sr}_{0.5}\text{MnO}_3$ .<sup>13</sup>

at  $T_{OO}/t_0 = 0.72$  and the transition from the ferromagnetic phase to the A-type AF one occurs at  $T_N$ . This transition is of the first order and the canted AF phase does not appear between the ferromagnetic and A-type AF phases. This sequential phase transition is caused by the thermal fluctuation of the orbital; as previously mentioned, the A-type AF state and the F-type orbital ordered one with  $d_{x^2-y^2}$  orbital are cooperatively stabilized at  $T = 0$ . With increasing  $T$ , the thermal fluctuation of orbital grows up and the hopping integral in the  $z$  direction becomes finite. As a result, the double exchange interaction in this direction overcomes the antiferromagnetic SE one and the ferromagnetic phase is stabilized. In the region II, the A-type AF ordering and the F-type orbital one with  $d_{x^2-y^2}$  orbital occur at the same temperature where the transition is of the first order as shown in Fig. 3(b). In both the regions I and II, the relation  $T_N \leq T_{OO}$  is satisfied. The first order transition at  $T_{OO}$  and this relation between  $T_{OO}$  and  $T_N$  originate from the breaking of the inversion symmetry of the system with respect to the orbital pseudo-spin operator, as discussed in the next section. The calculated results of the sequential phase transition in the region I well reproduce the experimental results observed in  $\text{Pr}_{0.5}\text{Sr}_{0.5}\text{MnO}_3$ <sup>13</sup> (the inset of Fig. 3 (a)). The first order transition at  $T_{OO}(= T_N)$  in the region II is consistent with the experiments in

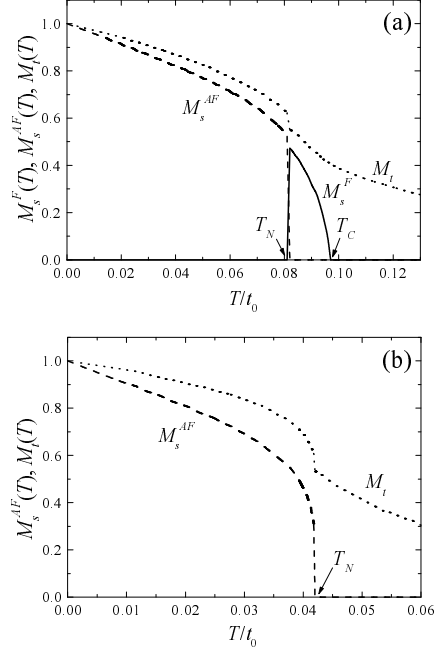


FIG. 4. Temperature dependences of the spin and orbital order parameters (a) at  $x = 0.725$  and (b) at  $x = 0.9$  in the tetragonal lattice. The solid, broken and dotted lines show the order parameters for the ferromagnetic structure ( $M_s^F$ ), the A-type AF one ( $M_s^{AF}$ ) and the F-type orbital ordered one ( $M_t$ ), respectively. The uniaxial anisotropy is introduced as  $t_0^{xy}/t_0^z = \sqrt{J_{AF}^{xy}/J_{AF}^z} = R$  with  $R = 1.2$  where  $t_0^{xy(z)}$  and  $J_{AF}^{xy(z)}$  are the hopping integral and the antiferromagnetic SE interaction in the  $xy$  plane (the  $z$  direction). The other parameter values are the same as those in Fig. 1.

$\text{Nd}_{0.45}\text{Sr}_{0.55}\text{MnO}_3$ <sup>13,14</sup> where the Mn-O band length in the  $z$  direction ( $xy$  plane) is confirmed to become short (long) at  $T_N$ .<sup>35</sup> It implies the F-type orbital ordering with  $d_{x^2-y^2}$  orbital as predicted from the present calculation.

In the actual compounds, where the A-type AF state is observed, the tetragonal lattice distortion is observed and the cubic symmetry is broken far above  $T_N$ .<sup>13,35</sup> We simulate this distortion by introducing the uniaxial anisotropy of the hopping integral and the SE interaction and investigate the phase transition. It is assumed that  $t_0^{xy}/t_0^z = \sqrt{J_{AF}^{xy}/J_{AF}^z} = R$  where  $t_0^{xy(z)}$  and  $J_{AF}^{xy(z)}$  are the hopping integral and the antiferromagnetic SE interaction in the  $xy$  plane ( $z$  direction). The temperature dependences of the spin and orbital order parameters at  $x = 0.725$  and  $x = 0.9$  with  $R = 1.2$  are shown in Figs. 4 (a) and (b), respectively. Due to the uniaxial anisotropy,  $M_t$  is finite above the orbital ordering temperature in the system with the cubic symmetry. It is worth to note that 1)  $T_N$  for the A-type AF state increases and 2) the transition at  $T_N$  is of the first order, although the discontinuity of  $M_s^{AF}$  is reduced. The latter is attributed to diminution of the change of  $M_t$  at  $T_N$ .

Finally, the magnetic field dependence of  $T_{OO}$  is shown

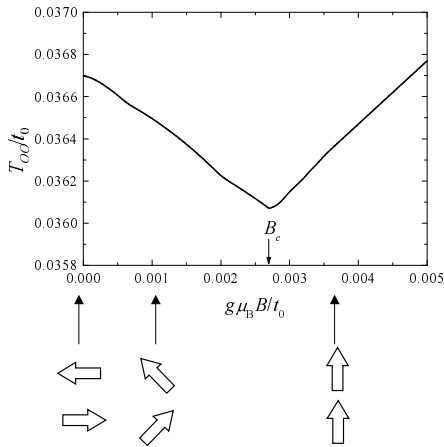


FIG. 5. Magnetic field dependence of the orbital ordering temperature at  $x = 0.9$  and schematic spin configurations. Parameter values are the same as those in Fig. 1.

in Fig. 5.  $T_{OO}$  decreases with applying the magnetic field in the region of  $g\mu_B B/t_0 < 0.0025$  where the nearest neighboring spins in the  $z$  direction are canted. The spins become parallel at  $g\mu_B B/t_0 = 0.0025$  termed  $B_c$ , and  $T_{OO}$  increases with increasing the magnetic field above  $B_c$ . The orbital ordered state below  $T_{OO}$  is of the F-type with  $d_{x^2-y^2}$  orbital and does not depend on magnitude of the magnetic field. Above and below  $B_c$ , the different mechanisms dominate the magnetic field dependence of  $T_{OO}$ ; in the region of  $B > B_c$ , the spin canting due to the magnetic field promotes the electron hopping in the  $z$  axis which weakens the orbital ordered state. On the other hand, above  $B_c$ , magnitude of the magnetic moment is enhanced by increasing of the magnetic field and the orbital ordered state associated with the ferromagnetic spin structure is stabilized. The magnetic field dependence of  $T_N$  for the A-type AF spin structure is recently measured in  $\text{Nd}_{0.45}\text{Sr}_{0.55}\text{MnO}_3$ .<sup>14</sup> It is experimentally shown that  $T_N$  gradually decreases with increasing the magnetic field. From the present calculation, it is predicted that this reduction of  $T_N$  is accompanied with that of  $T_{OO}$ , and with increasing the magnetic field furthermore,  $T_{OO}$  increases above the critical value of the field.

#### IV. FIRST ORDER TRANSITION AND ORBITAL DEGREE OF FREEDOM

As mentioned in Sect. III, several characteristics of the phase transitions in manganites are attributed to the unique properties of the orbital degree of freedom. In this section, we study analytically the phase transition by expanding the free energy with respect to the spin and orbital order parameters.<sup>24</sup> Let us consider the ferromagnetic and A-type AF spin structures and the F and G-type AF orbital ones. The expectation values of the Hamiltonian at finite temperature are calculated by

the mean field theory introduced in Sect. II and are expanded with respect to  $M_s$  and  $M_t$ . It is assumed that doped holes are introduced at the bottom of the band denoted by  $\varepsilon_k^l$  in Eq. (14). The explicit form of  $\langle \mathcal{H}_J \rangle_{st}$  is given by

$$\begin{aligned} \frac{\langle \mathcal{H}_J \rangle_{st}}{N} = & -\frac{(1-x)^2}{2} \sum_{l=x,y,z} \\ & \times \left\{ J_1(3 + \cos \Theta_l^s M_s^2)(1 - A_{2l} M_t^2) \right. \\ & + J_2(1 - \cos \Theta_l^s M_s^2) \\ & \left. \times (3 + A_{1l} M_t + A_{2l} M_t^2) \right\}, \quad (15) \end{aligned}$$

where

$$A_{1l} = 2(C_{Al} + C_{Bl}), \quad (16)$$

and

$$A_{2l} = C_{Al} C_{Bl}, \quad (17)$$

with  $C_{A(B)l} = \cos(\Theta_{A(B)}^t + 2\pi m_l/3)$  and  $(m_x, m_y, m_z) = (1, -1, 0)$ .  $\Theta_l^s$  ( $l = x, y, z$ ) is the relative angle between nearest neighboring spins in direction  $l$  and  $\Theta_{A(B)}^t$  is the angle of the orbital pseudo-spin in sublattice  $A(B)$ .  $\langle \mathcal{H}_t \rangle_{st}$  is proportional to the band width  $W$  of the spin- and orbital-less fermion as

$$\frac{\langle \mathcal{H}_t \rangle_{st}}{N} = -x \frac{W}{2}, \quad (18)$$

and is expanded with respect to  $M_s$  and  $M_t$  up to the orders of  $M_s^2$  and  $M_t^3$  as follows

$$\begin{aligned} \frac{\langle \mathcal{H}_t \rangle_{st}}{N} = & -t_0 x \frac{16}{3\pi^2} \sum_{l=x,y,z} \left( 1 + \frac{3}{5} \cos \Theta_l^s M_s^2 \right) \\ & \times \left( 1 + \alpha_{1l} M_t + \alpha_{2l} M_t^2 + \alpha_{3l} M_t^3 \right), \quad (19) \end{aligned}$$

where

$$\alpha_{1l} = \frac{2}{3}(C_{Al} + C_{Bl}), \quad (20)$$

$$\alpha_{2l} = \frac{2}{15}(1 - C_{Al}^2 - C_{Bl}^2) + \frac{4}{9}C_{Al}C_{Bl}, \quad (21)$$

and

$$\begin{aligned} \alpha_{3l} = & \frac{4}{105}(C_{Al}^3 + C_{Bl}^3) - \frac{4}{45}(C_{Al}^2 C_{Bl} + C_{Al} C_{Bl}^2) \\ & + \frac{1}{63}(C_{Al} + C_{Bl}). \quad (22) \end{aligned}$$

The detailed derivation of Eq. (19) is presented in Appendix. It is worth to note that the terms which are proportional to  $M_t$  or  $M_t^3$  appear in  $\langle \mathcal{H}_J \rangle_{st}$  and  $\langle \mathcal{H}_t \rangle_{st}$ . This is because the inversion symmetry in the system with respect to the orbital pseudo-spin is broken, i.e. the

free energy with  $T_z = 1/2$  is different from that with  $T_z = -1/2$ . This is highly in contrast to the spin case where the inversion symmetry with respect to the spin operator is preserved due to the time reversal symmetry in the system without magnetic field. Being based on Eqs. (15) and (19), we investigate the phase transition in the F and A-type AF spin structures in more detail.

*Ferromagnetic structure:* Eqs. (15) and (19) with the relation  $\Theta_l^s = 0$  for  $l = x, y$  and  $z$  are given by

$$\frac{\langle \mathcal{H}_J \rangle_{st}}{N} = -(1-x)^2 \frac{3}{8} J_1 (3 + M_s^2) (1 + B_2 M_t^2) - (1-x)^2 \frac{3}{8} J_2 (1 - M_s^2) (3 - B_2 M_t^2), \quad (23)$$

and

$$\frac{\langle \mathcal{H}_t \rangle_{st}}{N} = -t_0 x \frac{16}{\pi^2} \left( 1 + \frac{3}{5} M_s^2 \right) \times \left( 1 + \beta_2 M_t^2 + \beta_3 M_t^3 \right), \quad (24)$$

respectively, with

$$B_2 = -\frac{1}{2} \cos(\Theta_A^t - \Theta_B^t), \quad (25)$$

$$\beta_2 = \frac{2}{9} \cos(\Theta_A^t - \Theta_B^t), \quad (26)$$

and

$$\beta_3 = \frac{4}{105} (\cos^3 \Theta_A^t + \cos^3 \Theta_B^t) - \frac{1}{35} (\cos \Theta_A^t + \cos \Theta_B^t) - \frac{1}{45} \left( \cos(2\Theta_A^t + \Theta_B^t) + \cos(\Theta_A^t + 2\Theta_B^t) \right). \quad (27)$$

The terms being proportional to  $M_t$  vanish due to the cubic symmetry of the ferromagnetic spin structure. The coefficients  $B_2$  and  $\beta_2$  become the largest at  $\Theta_A^t = \Theta_B^t - \pi$  and at  $\Theta_A^t = \Theta_B^t$ , respectively. That is,  $\mathcal{H}_J$  and  $\mathcal{H}_t$  favor AF- and F-type orbital ordered states, respectively.

Let us focus on the term being proportional to  $M_t^3$  in  $\langle \mathcal{H}_t \rangle_{st}$ . In the case where this term is relevant, the orbital order-disorder transition is of the first order according to the Landau criterion in the phase transition. It corresponds to the transition at  $T_{OO}$  in the region of  $x > 0.25$  in Fig. 1 and is consistent with the first order transitions at the orbital ordering temperature observed in several manganites. On the other hand, the transition in the region of  $x < 0.25$  in Fig. 1 is of the second order. This is because 1) the term being proportional to  $M_t^3$  does not appear in  $\langle \mathcal{H}_J \rangle_{st}$ , and 2) in this hole concentration region, the G-type orbital ordered state with  $\Theta_A^t = \Theta_B^t - \pi$  is realized. The inversion symmetry with respect to the pseudo-spin operator is preserved, i.e.  $\beta_3 = 0$  in Eq. (27) in this orbital ordered state. The phase transition in this hole concentration region is discuss in more detail

in Sect. V. The first order transition in the cooperative Jahn-Teller system and its relation to the terms proportional to  $Q^3$ , where  $Q$  indicates the normal mode of a  $\text{MnO}_6$  octahedron, was discussed in Ref. 37.

The parameter  $\beta_3$  becomes the largest at  $\Theta_A^t = \Theta_B^t = (2n+1)\pi/3$  with  $n = (1, 2, 3)$  and determines the orbital state uniquely. With taking into account  $\beta_2$  together with  $\beta_3$ ,  $\langle \mathcal{H}_t \rangle_{st}$  favors the F-type orbital ordered state with  $d_{x^2-y^2}$ ,  $d_{y^2-z^2}$  and  $d_{z^2-x^2}$  (the so-called leaf-type orbital) rather than  $d_{3z^2-r^2}$ ,  $d_{3x^2-r^2}$  and  $d_{3y^2-r^2}$  (the so-called cigar-type one). Since the band width in the F-type orbital ordered state at  $T = 0$  does not depend on types of the orbital, the thermal fluctuation stabilises the leaf-type orbital; the F-type orbital ordered state with  $d_{x^2-y^2}$  ( $d_{3z^2-r^2}$ ) mixes with the AF-type one with  $(d_{3x^2-r^2}/d_{3y^2-r^2})$  ( $(d_{y^2-z^2}/d_{z^2-x^2})$ ) through the thermal fluctuation. The band width in the  $(d_{3x^2-r^2}/d_{3y^2-r^2})$  state is  $5t_0$  which is larger than that in the  $(d_{y^2-z^2}/d_{z^2-x^2})$  one ( $3t_0$ ). The smaller band width in the latter state is attributed to the fact that the hopping integral in the  $xy$  plane is zero in this orbital state.

*A-type AF structure:* In this spin structure,  $\langle \mathcal{H}_J \rangle_{st}$  and  $\langle \mathcal{H}_t \rangle_{st}$  with  $\Theta_x^s = \Theta_y^s = 0$  and  $\Theta_z^s = \pi$  are given by

$$\frac{\langle \mathcal{H}_J \rangle_{st}}{N} = (1-x)^2 \frac{1}{16} (J_1 D_1 + J_2 D_2), \quad (28)$$

with

$$D_1 = -18 - 2M_s^2 + 9 \cos(\Theta_A^t - \Theta_B^t) M_t^2 + \left( 3 \cos(\Theta_A^t - \Theta_B^t) - 2 \cos \Theta_A^t \cos \Theta_B^t \right) M_s^2 M_t^2, \quad (29)$$

and

$$D_2 = -18 + 6M_s^2 - 3 \cos(\Theta_A^t - \Theta_B^t) M_t^2 - 4(\cos \Theta_A^t + \cos \Theta_B^t) M_s^2 M_t + \left( 3 \cos(\Theta_A^t - \Theta_B^t) - 2 \cos \Theta_A^t \cos \Theta_B^t \right) M_s^2 M_t^2, \quad (30)$$

and

$$\frac{\langle \mathcal{H}_t \rangle_{st}}{N} = -t_0 x \left( \frac{16}{\pi^2} \right) \times \left( 1 + \frac{1}{5} M_s^2 + \gamma_1 M_s^2 M_t + \beta_2 M_t^2 + \beta_3 M_t^3 \right), \quad (31)$$

with

$$\gamma_1 = -\frac{4}{15} (\cos \Theta_A^t + \cos \Theta_B^t), \quad (32)$$

respectively. The most remarkable difference of the results in the A-type AF structure from that in the ferromagnetic one is the terms being proportional to  $M_s^2 M_t$ . The origin of these terms is the anisotropic spin structure in the A-type AF state which breaks the cubic symmetry in the system. Because of these terms, the order parameter of the A-type AF state acts as a magnetic field on the orbital pseudo-spin space and the relation  $T_{OO} \geq T_N$

is derived. This relation is seen in the present phase diagram (Fig. 1) and also in the experimental results in several manganites.

Now we focus on these terms being proportional to  $M_t M_s^2$ . At  $x = 0$  where  $\mathcal{H}_J$  is dominant, the AF-type orbital ordered states with  $(\Theta^t/\Theta^t + \pi)$  for any  $\Theta^t$  is realized above  $T_N$ . Below  $T_N$ , the term being proportional to  $M_s^2 M_t$  becomes relevant and the orbital state is uniquely determined as  $(\Theta^t / -\Theta^t)$  with

$$\Theta^t = \cos^{-1} \frac{4J_2 M_s^2}{3(3J_1 - J_2)M_t + (J_1 + J_2)M_s^2 M_t}. \quad (33)$$

With decreasing temperature below  $T_N$ ,  $\Theta^t$  continuously changes from  $\pi/2$  at  $T_N$  to  $\cos^{-1}\{2J_2/(5J_1 - J_2)\}$  at  $T = 0$ . This orbital state favors the antiferromagnetic interaction in the  $z$  direction in this spin structure. In the highly doped region where  $\mathcal{H}_t$  is dominant, the term  $\gamma_1 M_s^2 M_t$  in Eq. (31) favors the F-type orbital ordered state with  $\Theta_A^t = \Theta_B^t = \pi$  which corresponds to the state with  $d_{x^2-y^2}$ , as mentioned in the previous section. The terms being proportional to  $M_s^2 M_t$  also appear in the C-type AF spin structure where the relation  $T_{OO} \geq T_N$  is derived. The coefficients of the term in  $\langle \mathcal{H}_J \rangle_{st}$  and  $\langle \mathcal{H}_t \rangle_{st}$  are given by  $J_2(1-x)^2(\cos \Theta_A^t + \cos \Theta_B^t)/2$  and  $-t_0 x 32(\cos \Theta_A^t + \cos \Theta_B^t)/(5\pi^2)$  which favor the G-type with  $(d_{3z^2-r^2}/d_{x^2-y^2})$  and F-type with  $d_{3z^2-r^2}$  orbital ordered states, respectively.

## V. SUMMARY AND DISCUSSION

In this paper, we study roles of the orbital degree of freedom in phase transition in perovskite manganites. The effective Hamiltonian which includes the orbital degree of freedom as well as the spin and charge ones is utilized and the mean field theory at finite temperature and carrier concentration is adopted. Through both the numerical and analytical calculations based on this theory, it is revealed that several characteristics of the phase transition observed in manganites originate from the unique properties of the orbital degree of freedom. The obtained results are summarized as follows: 1) The orbital order-disorder transition is of the first order in the wide region of  $x$ , and  $T_N$  for the anisotropic spin structure, such as the A- and C-type AF ones, is lower than  $T_{OO}$ . Both the results originate from the fact that the inversion symmetry in the system is broken with respect to the orbital pseudo-spin operator and the terms being proportional to  $M_s^2 M_t$  and  $M_t^3$  exist in the free energy. These results are consistent with the phase transition observed in  $\text{Pr}_{0.5}\text{Sr}_{0.5}\text{MnO}_3$  and  $\text{Nd}_{0.45}\text{Sr}_{0.55}\text{MnO}_3$ <sup>13,14,35</sup> where the A-type AF state with  $d_{x^2-y^2}$  orbital ordered one appears. The calculated results may be also applicable to the orbital ordering associated with the CE-type AF one which is experimentally confirmed to be of the first order transition in  $\text{Pr}_{1-x}\text{Ca}_x\text{MnO}_3$ .<sup>36</sup> In the present calculation, the phase transition at  $T_{OO}$  in the

region of  $x < 0.25$  is of the second order as shown in Fig. 1. With taking into account the higher order coupling between the pseudo-spin and the Jahn-Teller type distortion in a  $\text{MnO}_6$  octahedron and the anharmonic term of the potential energy for the lattice distortion, the phase transition changes from the second order to the first one.<sup>37</sup> However, since the phase transition experimentally observed in  $\text{LaMnO}_3$  at 780K is almost of the second order,<sup>11,12</sup> it is supposed that the effects are small or are canceled out with each other in the compound. 2) The relation  $T_C > T_{OO}$  is satisfied in highly hole doped region ( $x > 0.1$ ). This is because gain of the kinetic energy of electrons accompanied with the orbital ordering is lower than that with the ferromagnetic one due to the hopping integral between different kinds of orbital unlike spin case. 3) In the region where  $T_{OO}$  and  $T_C$  are close with each other, the novel phase transition is brought about due to the coupling between the spin and orbital degrees of freedom. The magnetization is enhanced below  $T_{OO}$  and  $T_{OO}$  increases by applying the magnetic field. These results well explain the unique experimental results observed in  $\text{La}_{0.88}\text{Sr}_{0.12}\text{MnO}_3$ . 4) The sequential phase transition from the A-type AF phase to the ferromagnetic one with increasing  $T$  is caused by the thermal fluctuation of the orbital from the  $d_{x^2-y^2}$  orbital ordered states. The ferromagnetic interaction in the  $z$  axis becomes finite due to the orbital fluctuation.

## ACKNOWLEDGMENTS

The authors would like to thank Y. Endoh, K. Hirota, H. Nojiri and Y. Murakami for their valuable discussions. This work was supported by CREST (Core Research for Evolutional Science and Technology Corporation) Japan, NEDO (New Energy Industrial Technology Development Organization) Japan, and Grant-in-Aid for Scientific Research Priority Area from the Ministry of Education, Science and Culture of Japan. S. O. acknowledges the financial support of JSPS Research Fellowship for Young Scientists. Part of the numerical calculation was performed in the HITACS-3800/380 supercomputing facilities in IMR, Tohoku University.

## APPENDIX: EXPANSION OF $\langle \mathcal{H}_t \rangle_{st}$

In this appendix, we present derivation of Eq. (19), i.e. the expansion of  $\langle \mathcal{H}_t \rangle_{st}$  with respect to the spin and orbital order parameters. We start from Eq. (18) where the band width  $W$  is calculated from Eq. (13) as follows

$$W = 2 \sum_{\delta} I_{\delta}^s I_{\delta}^t, \quad (A1)$$

where

$$I_{\delta}^s = \sum_{\sigma} \langle |z_{i\sigma}^{s*} z_{j\sigma}^s| \rangle_s, \quad (A2)$$



and

$$I_{\delta}^t = \sum_{\sigma} \langle |z_{i\gamma}^{t*} t_{ij}^{\gamma\gamma'} z_{j\gamma'}^t| \rangle_t. \quad (\text{A3})$$

Here,  $\delta$  indicates a vector connecting site  $i$  and its nearest neighboring site  $j$ . The spin part  $I_{\delta}^s$  has the same form with Eq. (27) in Ref. 24 and is given by

$$I_{\delta}^s = \frac{2}{3} \left( 1 + \frac{3}{5} \cos \Theta_{\delta}^s M_s^2 \right), \quad (\text{A4})$$

where  $\Theta_{\delta}^s$  is the relative angle between spins at site  $i$  and site  $j$  and the relation  $M_s = \lambda^s/3 + O(\lambda^{s3})$  is used. As for the orbital part, we present the derivation of  $I_{\delta}^t$  with  $\delta = \pm a\hat{z}$  termed  $I_z^t$  where  $a$  and  $\hat{z}$  indicate a cell parameter of the cubic perovskite lattice and the unit vector in the  $z$  direction, respectively.  $I_{\delta}^t$  with  $\delta = \pm a\hat{x}(\hat{y})$  is given by  $I_z^t$  where  $\Theta_i^t$  is replaced by  $\Theta_i^t + 2\pi/3$  ( $\Theta_i^t - 2\pi/3$ ).  $I_z^t$  is calculated as

$$\begin{aligned} I_z^t &= t_0 \left\langle \left| \cos \frac{\theta_i^t}{2} \cos \frac{\theta_j^t}{2} \right| \right\rangle_t \\ &= \frac{t_0}{\nu^{t2}} \int_0^{2\pi} d\delta\theta_i \int_0^{2\pi} d\delta\theta_j e^{\lambda^t (\cos \delta\theta_i + \cos \delta\theta_j)} \\ &\quad \times \left| \cos \frac{\Theta_i^t + \delta\theta_i}{2} \cos \frac{\Theta_j^t + \delta\theta_j}{2} \right|, \end{aligned} \quad (\text{A5})$$

where  $\delta\theta_i = \theta_i^t - \Theta_i^t$ . The right hand side in Eq. (A5) is expanded with respect to  $\lambda^t$  up to the order of  $O(\lambda^{t3})$  as follows

$$\begin{aligned} I_z^t &= \frac{t_0}{(2\pi)^2} \left( 1 - \frac{\lambda^{t2}}{4} \right)^2 \\ &\quad \times \left( \zeta_{i0} + \zeta_{i1}\lambda^t + \frac{\zeta_{i2}}{2!}\lambda^{t2} + \frac{\zeta_{i3}}{3!}\lambda^{t3} \right) \\ &\quad \times \left( \zeta_{j0} + \zeta_{j1}\lambda^t + \frac{\zeta_{j2}}{2!}\lambda^{t2} + \frac{\zeta_{j3}}{3!}\lambda^{t3} \right), \end{aligned} \quad (\text{A6})$$

where  $\zeta_{in}$  ( $n = 0 \sim 3$ ) are given by

$$\zeta_{i0} = 4, \quad (\text{A7})$$

$$\zeta_{i1} = \frac{4}{3} \cos \Theta_i^t, \quad (\text{A8})$$

$$\zeta_{i2} = \frac{4}{15} (8 - \cos^2 \Theta_i^t), \quad (\text{A9})$$

and

$$\zeta_{i3} = \frac{4}{35} (\cos^3 \Theta_i^t + 8 \cos \Theta_i^t). \quad (\text{A10})$$

The relation  $\nu^t = 2\pi(1 + \frac{1}{4}\lambda^{t2}) + O(\lambda^{t4})$  is used. In the G-type orbital ordered state considered in Sect. III,  $\Theta_i^t$  in the above formulas is replaced by  $\Theta_{A(B)}^t$ , when site  $i$  belongs to the orbital sublattice  $A(B)$ . By utilizing the relation  $M_t = \lambda^t/2 - \lambda^{t3}/16 + O(\lambda^{t5})$ , Eq. (19) is derived.

- <sup>1</sup> K. Chahara, T. Ohono, M. Kasai, Y. Kanke, and Y. Kozono, Appl. Phys. Lett. **62**, 780 (1993).
- <sup>2</sup> R. von Helmolt, J. Wecker, B. Holzapfel, L. Schultz, and K. Samwer, Phys. Rev. Lett. **71**, 2331 (1993).
- <sup>3</sup> Y. Tokura, A. Urushibara, Y. Moritomo, T. Arima, A. Asamitsu, G. Kido, and N. Furukawa, J. Phys. Soc. Jpn. **63**, 3931 (1994).
- <sup>4</sup> S. Jin, T. H. Tiefel, M. McCormack, R. A. Fastnacht, R. Ramesh, and L. H. Chen, Science **264**, 413 (1994).
- <sup>5</sup> Y. Tomioka, A. Asamitsu, Y. Moritomo, and Y. Tokura J. Phys. Soc. Jpn. **64**, 3626 (1995).
- <sup>6</sup> P. Schiffer, A. P. Ramirez, W. Bao, and S. -W. Cheong, Phys. Rev. Lett. **75**, 3336 (1995).
- <sup>7</sup> A. J. Millis, P. B. Littlewood, and B. I. Shraiman, Phys. Rev. Lett. **74**, 5144 (1995).
- <sup>8</sup> J. B. Goodenough, Phys. Rev. **100**, 564 (1955), and in *Progress in Solid State Chemistry*, edited by H. Reiss (Pergamon, London, 1971), Vol. 5.
- <sup>9</sup> J. Kanamori, J. Phys. Chem. Sol. **10**, 87 (1959).
- <sup>10</sup> G. Matsumoto, J. Phys. Soc. Jpn. **29**, 606 (1970).
- <sup>11</sup> J. Rodriguez-Carvajal, M. Hennion, F. Moussa, and A. H. Moudden, Phys. Rev. B **57**, R3189 (1998).
- <sup>12</sup> Y. Murakami, J. P. Hill, D. Gibbs, M. Blume, I. Koyama, M. Tanaka, H. Kawata, T. Arima, Y. Tokura, K. Hirota, and Y. Endoh, Phys. Rev. Lett. **81**, 582 (1998).
- <sup>13</sup> H. Kawano, R. Kajimoto, H. Yoshizawa, Y. Tomioka, H. Kuwahara, and Y. Tokura, Phys. Rev. Lett. **78**, 4253 (1997).
- <sup>14</sup> H. Kuwahara, T. Okuda, Y. Tomioka, A. Asamitsu, and Y. Tokura, Phys. Rev. Lett. **82**, 4316 (1999) and Mat. Res. Soc. Sym. Proc. **494**, 83 (1998).
- <sup>15</sup> Y. Tomioka and Y. Tokura, (unpublished).
- <sup>16</sup> T. Akimoto, Y. Maruyama, Y. Moritomo, A. Nakamura, K. Hirota, K. Ohoyama, and M. Ohashi, Phys. Rev. B **57**, R5594 (1998).
- <sup>17</sup> S. Ishihara, J. Inoue, and S. Maekawa, Physica C **263**, 130 (1996), and Phys. Rev. B **55**, 8280 (1997).
- <sup>18</sup> J. C. Slater, and G. F. Koster, Phys. Rev. **94**, 1498 (1954); W. A. Harrison, in *Electronic Structure and the Properties of Solids, The Physics of the Chemical Bond*, W.H. Freeman and Company, San Francisco (1980).
- <sup>19</sup> Y. Endoh, K. Hirota, S. Ishihara, S. Okamoto, Y. Murakami, A. Nishizawa, T. Fukuda, H. Kimura, H. Nojiri, K. Kaneko, and S. Maekawa, Phys. Rev. Lett. **82**, 4328 (1999).
- <sup>20</sup> L. M. Roth, Phys. Rev. **149**, 306 (1966).
- <sup>21</sup> K. I. Kugel and D. I. Khomskii, JETP Lett. **15**, 446 (1972).
- <sup>22</sup> M. Cyrot, and C. Lyon-Caen, Le J. de Physique **36**, 253 (1975).
- <sup>23</sup> S. Inagaki, J. Phys. Soc. Jpn. **39**, 596 (1975).
- <sup>24</sup> P. G. de Gennes, Phys. Rev. **118**, 141 (1960).
- <sup>25</sup> S. Okamoto, S. Ishihara, and S. Maekawa, (unpublished) cond-mat/9902266.
- <sup>26</sup> S. Ishihara, M. Yamanaka, and N. Nagaosa, Phys. Rev. B **56**, 686 (1997).
- <sup>27</sup> S. Ishihara, S. Okamoto, and S. Maekawa, J. Phys. Soc. Jpn. **66**, 2965 (1997).
- <sup>28</sup> R. Maezono, S. Ishihara, and N. Nagaosa, Phys. Rev. B **57**, R13993 (1998), *ibid.* **58**, 11583 (1998).
- <sup>29</sup> L. Sheng and C. S. Ting, (unpublished) cond-mat/9812374.

- <sup>30</sup> Y. Tokura, J. Appl. Phys. **79**, 5288 (1996).
- <sup>31</sup> H. Nojiri, K. Kaneko, M. Motokawa, K. Hirota, Y. Endoh, and K. Takahashi, Phys. Rev. B **60**, 4142 (1999).
- <sup>32</sup> R. Senis, V. Laukhin, B. Martnez, J. Fontcuberta, X. Obradors, A. A. Arsenov, and Y. M. Mukovskii, Phys. Rev. B **57**, 14680 (1998).
- <sup>33</sup> K. Ghosh, R. L. Greene, S. E. Lofland, S. M. Bhagat, S. G. Karabashev, D. A. Shulyatev, A. A. Arsenov, and Y. Mukovskii, Phys. Rev. B **58**, 8206 (1998).
- <sup>34</sup> S. Uhlenbruck, R. Teipen, R. Klingeler, B. Büchner, O. Friedt, M. Hücker, H. Kierspel, T. Niemöller, L. Pinsard, A. Revolevshi, and R. Gross, Phys. Rev. Lett. **82**, 185 (1999).
- <sup>35</sup> R. Kajimoto, H. Yoshizawa, H. Kawano, H. Kuwahara, Y. Tokura, K. Ohoyama, and M. Ohashi, Phys. Rev. B **60** (Oct. 1) (1999) (to be published).
- <sup>36</sup> Y. Tomioka, A. Asamitsu, H. Kuwahara, Y. Moritomo, and Y. Tokura, Phys. Rev. B **53**, R1689 (1996).
- <sup>37</sup> M. Kataoka, and J. Kanamori, J. Phys. Soc. Jpn. **32**, 113 (1972).